SUPPLEMENTARY INFORMATION FOR:

Significant Relaxation of SARS-CoV-2-Targeted Non-Pharmaceutical Interventions Will Result in Profound Mortality: A New York State Modelling Study

BENJAMIN U. HOFFMAN, MD, PHD[1,2]

[1]Vagelos College of Physicians and Surgeons, Columbia University, New York, NY

[2]Corresponding Author: Buh2003@cumc.columbia.edu

104 Haven Avenue, Room 1103

New York, NY 10032

SUPPLEMENTARY METHODS

System of Ordinary Differential Equations

$$\frac{dS}{dt} = -\chi(t)\rho\frac{\beta S}{N}(U + I) - \alpha(t)S + \zeta(t)P + \frac{\pi}{1-\tau}\left(R_U + R_Q + R_H\right)$$

$$\frac{dE}{dt} = \chi(t)\rho\frac{\beta S}{N}(U + I) - \gamma E$$

$$\frac{dI}{dt} = \gamma E - \nu I - \theta I - \delta I$$

$$\frac{dU}{dt} = \nu I - \phi U$$

$$\frac{dQ}{dt} = \theta I - \omega Q$$

$$\frac{dH}{dt} = \delta I - \lambda(t)H - \kappa(t)H$$

$$\frac{dR_U}{dt} = \phi U - \frac{\pi}{1-\tau}R_U$$

$$\frac{dR_Q}{dt} = \omega Q - \frac{\pi}{1-\tau}R_Q$$

$$\frac{dR_H}{dt} = \lambda(t)H - \frac{\pi}{1-\tau}R_H$$

$$\frac{dD}{dt} = \kappa(t)H$$

$$\frac{dP}{dt} = \alpha(t)S - \zeta(t)P$$

Parameter estimation

Parameters of the model were estimated with global optimization, using the particle swarm algorithm with post-hoc large-scale constrained non-linear minimization ("fmincon") implemented with an iterative sequential quadratic programming algorithm ("sqp") in Matlab (**Tables S1-2**) [1, 2]. Confidence intervals were estimated by bootstrapping the "fmincon" optimization algorithm with random lognormal gaussian noise applied to the SARS-CoV-2 sample data.

Sensitivity analysis and goodness of fit

The sensitivity of the model was estimated with two methods. First, bivariate sensitivity analysis was performed, where pairs of parameters were varied while other parameters were held at best-fit values. The model was simulated with each combination, and the total deaths of the simulation estimated by September 1st, 2020 were evaluated (**Figure S2**). Next, a global sensitivity analysis was performed to evaluate the first-order global sensitivity coefficients using the Sobol's method, with samples selected through 10000 iterations of a quasi-random Monte Carlo Simulation (**Figure S3**) [3]. Goodness of fit was evaluated by analyzing the residuals of the fit, which reveal an approximately normal distribution (**Figure S4**).

Reproductive number

The basic reproductive number (R_0) of the system was solved for using the next-generation matrix method (see, *Supplementary Methods*) [4, 5]:

$$R_0 = \frac{\chi\rho\beta}{\nu+\delta+\theta}\left(1+\frac{\nu}{\phi}\right)$$

The instantaneous effective reproductive number ($R(t)$) was solved for with the following equation:

$$R(t) = \frac{R_o S}{N}$$

During the initial period of the outbreak of an infectious disease, there is relative lack of testing capacity compared to the prevalence of the pathogen. As testing capacity increases, one can confound this improved detection rate with rapid transmission of the pathogen. In order to avoid this, the peak reproductive number was estimated after the daily rate of change in the ratio of positive tests to confirmed tests was negative for 7 consecutive days. SARS-CoV-2 testing data was sourced from the NYSDOH [6].

Basic Reproductive Number Proof

To solve for the basic reproductive number, first the system was evaluated at the disease-free equilibrium:

$$\left(S_0, E_0, I_0, U_0, Q_0, H_0, R_{U_0}, R_{Q_0}, R_{H_0}, D_0, P_0\right) = (N, 0,0,0,0,0,0,0,0,0,0)$$

Next, a sub-model of the system was made where:

$$\frac{d\vec{x}}{dt} = F(\vec{x}) - V(\vec{x})$$

$$= F(\vec{x}) - (V^-(\vec{x}) - V^+(\vec{x}))$$

$$= \begin{bmatrix} \frac{\chi\rho\beta S(U+I)}{N} \\ 0 \\ 0 \\ 0 \\ 0 \end{bmatrix} - \begin{bmatrix} \gamma E \\ \nu I + \delta I + \theta I - \gamma E \\ \phi U - \nu I \\ \omega Q - \theta I \\ \lambda(t)H + \kappa(t)H - \delta I \end{bmatrix}$$

$$= \begin{bmatrix} \frac{\chi\rho\beta S(U+I)}{N} - \gamma E \\ \gamma E - \nu I - \delta I - \theta I \\ \nu I - \phi U \\ \theta I - \omega Q \\ \delta I - \lambda(t)H - \kappa(t)H \end{bmatrix}$$

Then, the Jacobian Matrix of the sub-model was evaluated at the disease-free equilibrium:

$$J\left(S_0, E_0, I_0, U_0, Q_0, H_0, R_{U_0}, R_{Q_0}, R_{H_0}, D_0, P_0\right) = \begin{bmatrix} -\gamma & \chi\rho\beta & \chi\rho\beta & 0 & 0 \\ \gamma & -\nu-\theta-\delta & 0 & 0 & 0 \\ 0 & \nu & -\phi & 0 & 0 \\ 0 & \theta & 0 & -\omega & 0 \\ 0 & \delta & 0 & 0 & -\lambda(t)-\kappa(t) \end{bmatrix}$$

Thus, the next generation matrix was:

$$FV^{-1} = \begin{bmatrix} \frac{\chi\rho\beta}{\nu+\delta+\theta}(1+\frac{\nu}{\phi}) & \frac{\chi\rho\beta}{\nu+\delta+\theta}(1+\frac{\nu}{\phi}) & \frac{\chi\rho\beta}{\phi} & 0 & 0 \\ 0 & 0 & 0 & 0 & 0 \\ 0 & 0 & 0 & 0 & 0 \\ 0 & 0 & 0 & 0 & 0 \\ 0 & 0 & 0 & 0 & 0 \end{bmatrix}$$

The basic reproductive number R_0 is the largest eigenvalue of the next generation matrix. Thus:

$$R_0 = \frac{\chi\rho\beta}{\nu+\delta+\theta}(1+\frac{\nu}{\phi})$$

Table S1. Fixed Parameters

Parameter	Definition	Value	Details
ρ	Population Density (1000s people per mi^2)	2.726	[7]
γ^{-1}	Average incubation period	3	[8-10]
δ^{-1}	Average time to hospitalization	5	[11]
θ	Effective rate of non-hospitalized quarantine	0.57	Derived from source data [6, 12].
ν	Effective rate of undocumented infections	2.25	Undocumented rate of 0.75 constrained to g and d [13-15].
τ	Fraction non-immune	0.30 (varied in some simulations)	[16, 17]
π	Average duration of immunity	5 years (varied in some simulations)	[16, 17]

Table S2. Fit Parameters

Parameter	Definition	Value	95% Confidence Interval
α	Effective protection rate	0.105	(0.095, 0.112)
ζ	Effective protection leak rate	0.016	(0.012,0.018)
β	Effective contact rate	0.281	(0.269, 0.285)
λ	Initial effective hospitalized recovery rate	0.174	(0.166, 0.200)
ε	Hospitalized recovery rate improvement rate constant	0.226	(0.191,0.312)
σ	Efficacy of improved recovery rate	0.513	(0.405,0.575)
κ	Initial effective death rate	0.098	(0.092, 0.114)
ψ	Death rate improvement rate constant	0.404	(0.313, 0.438)
μ	Efficacy of reduced death rate	2.75	(2.465, 3.096)

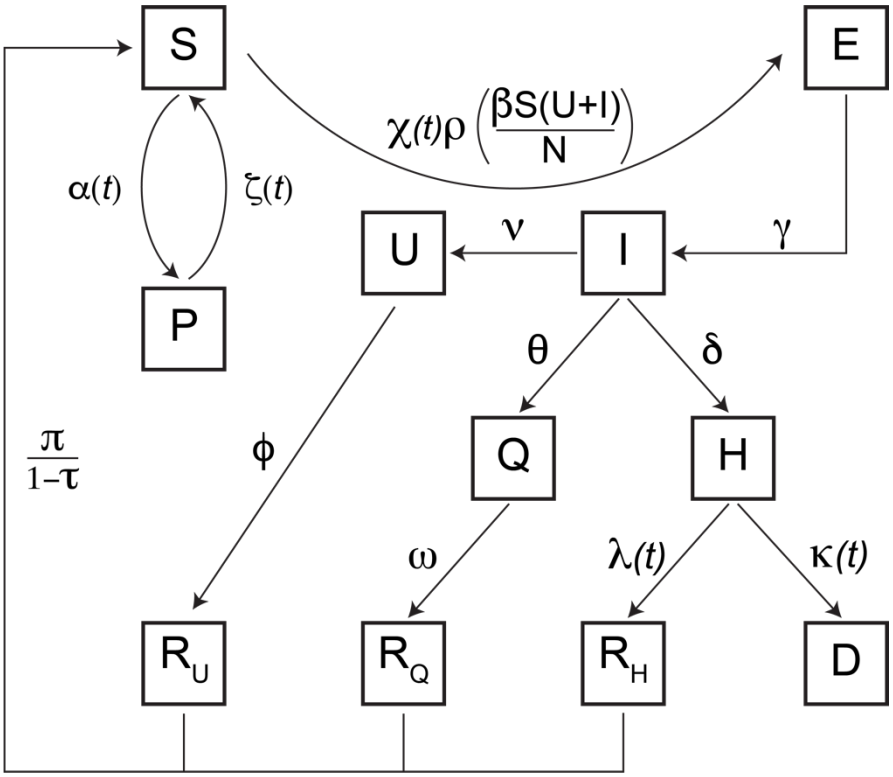

Figure S1. Schematic of SARS-CoV-2 transmission model. S (susceptible), E (exposed individuals), I (infected), U (undocumented), Q (quarantined), H (hospitalized), R_U (recovered undocumented), R_Q (recovered quarantined), R_H (recovered hospitalized), D (dead), and P (protected).

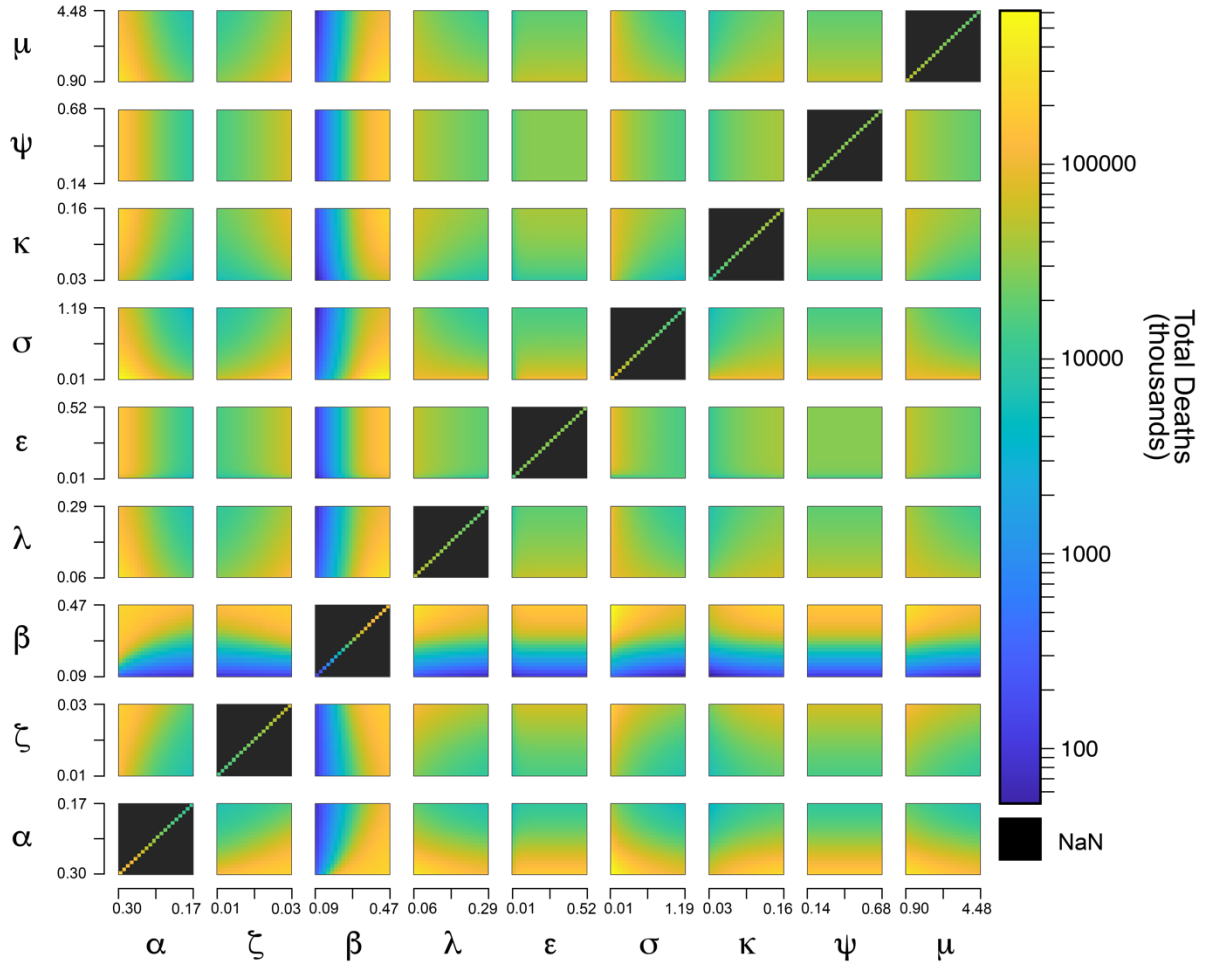

Figure S2. Bivariate sensitivity analysis of model parameters with respect to total deaths, related to Figure 1.

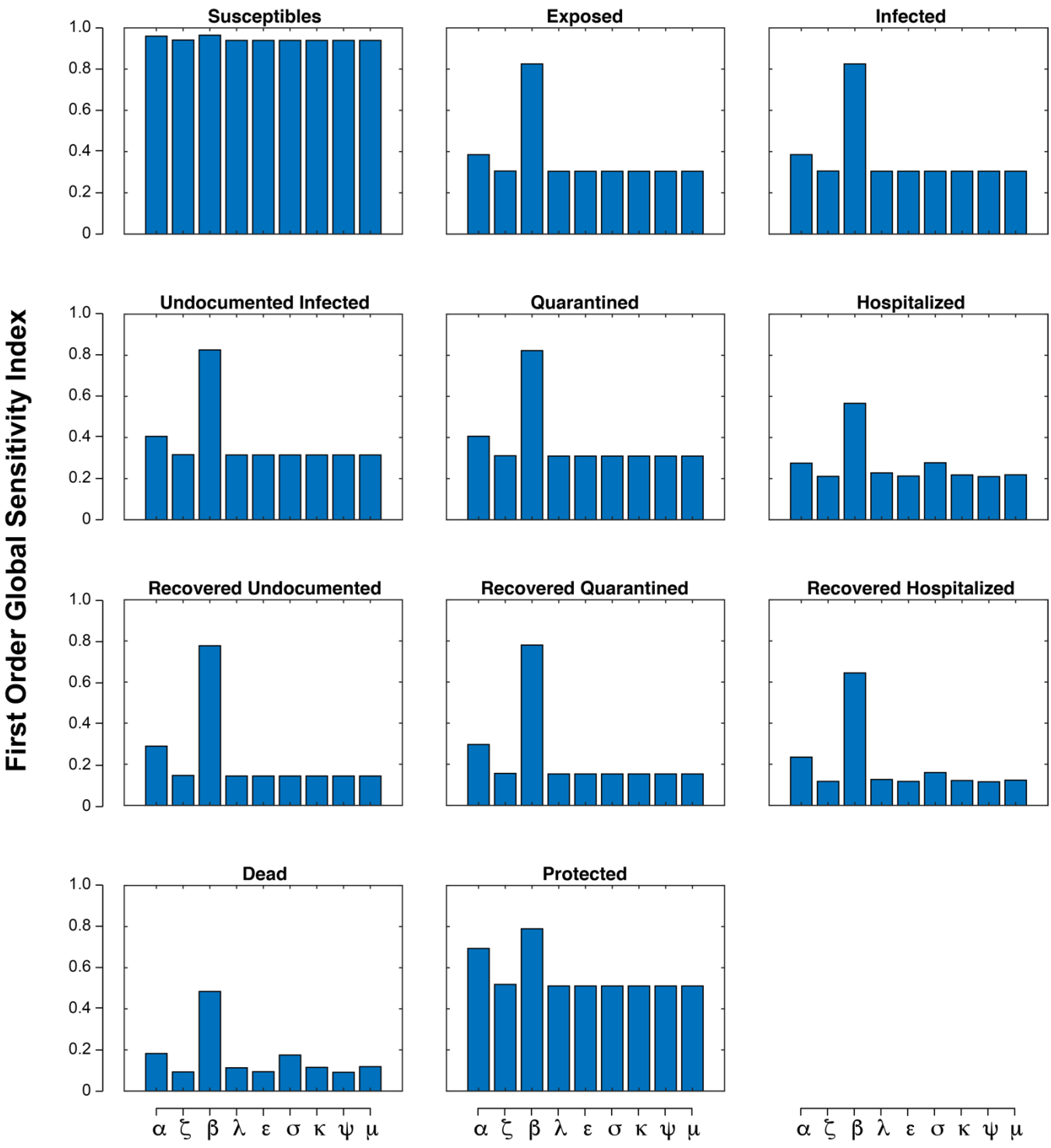

Figure S3. Global sensitivity analysis of model parameters with respect to total deaths, related to Figure 1

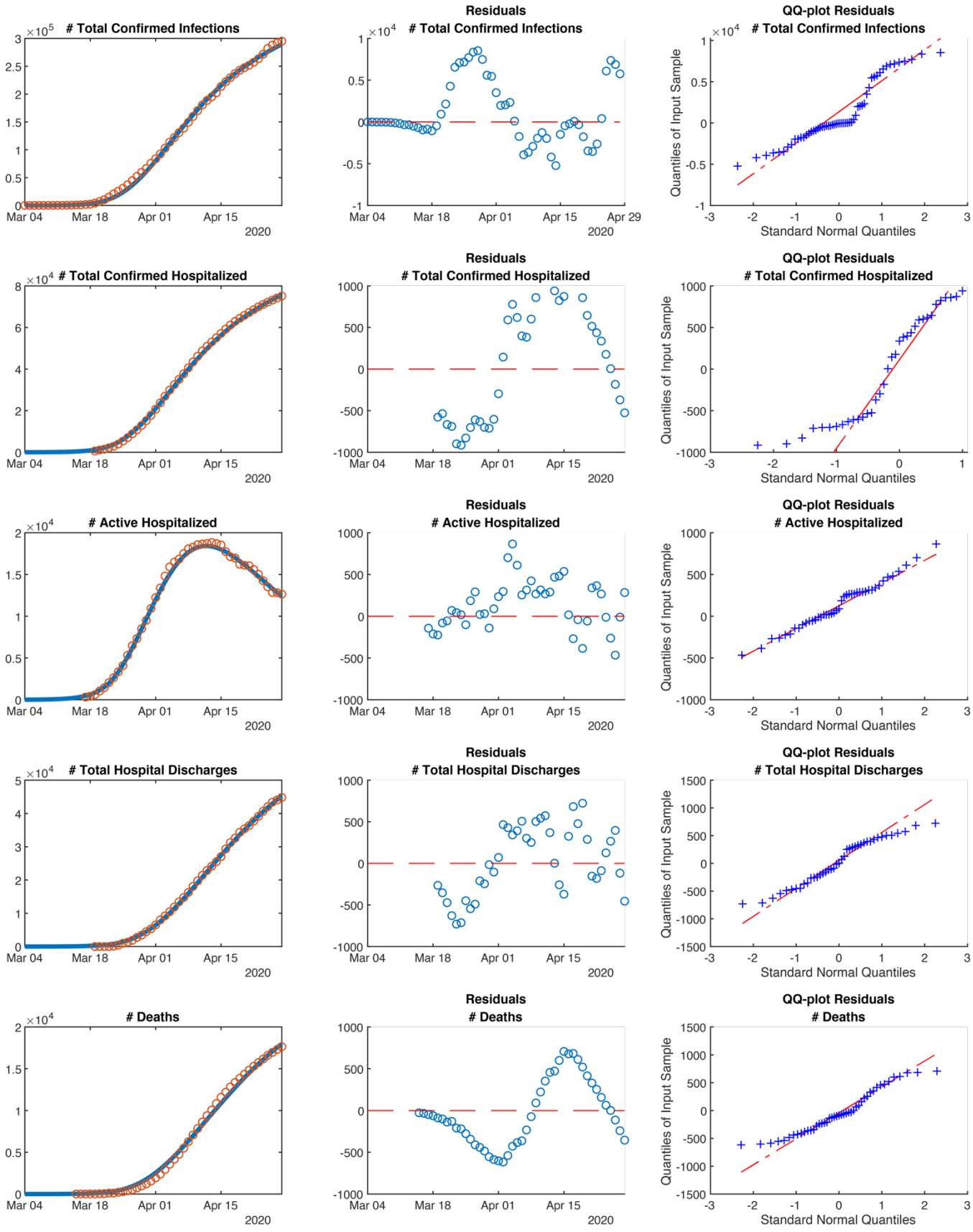

Figure S4. Goodness of fit analysis, related to Figure 1

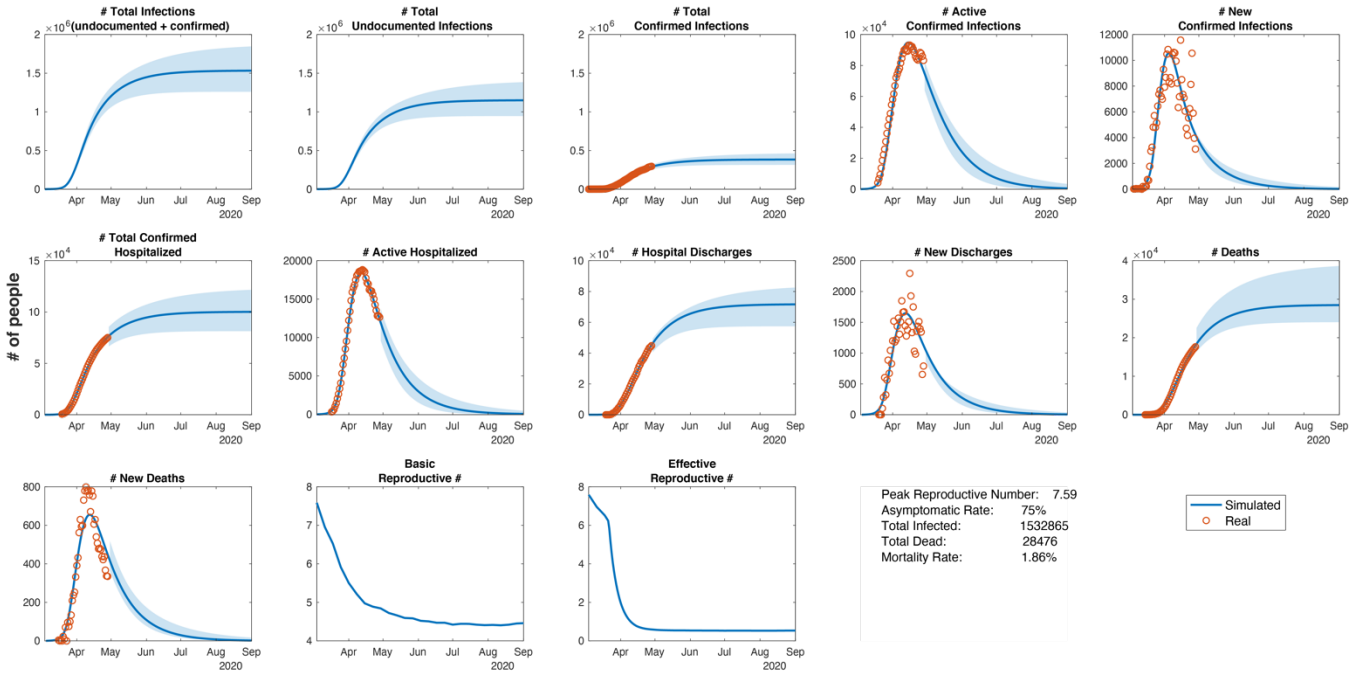

Figure S5. Undocumented infections drive SARS-CoV-2 transmission, comprehensive model outputs, related to Figure 1.

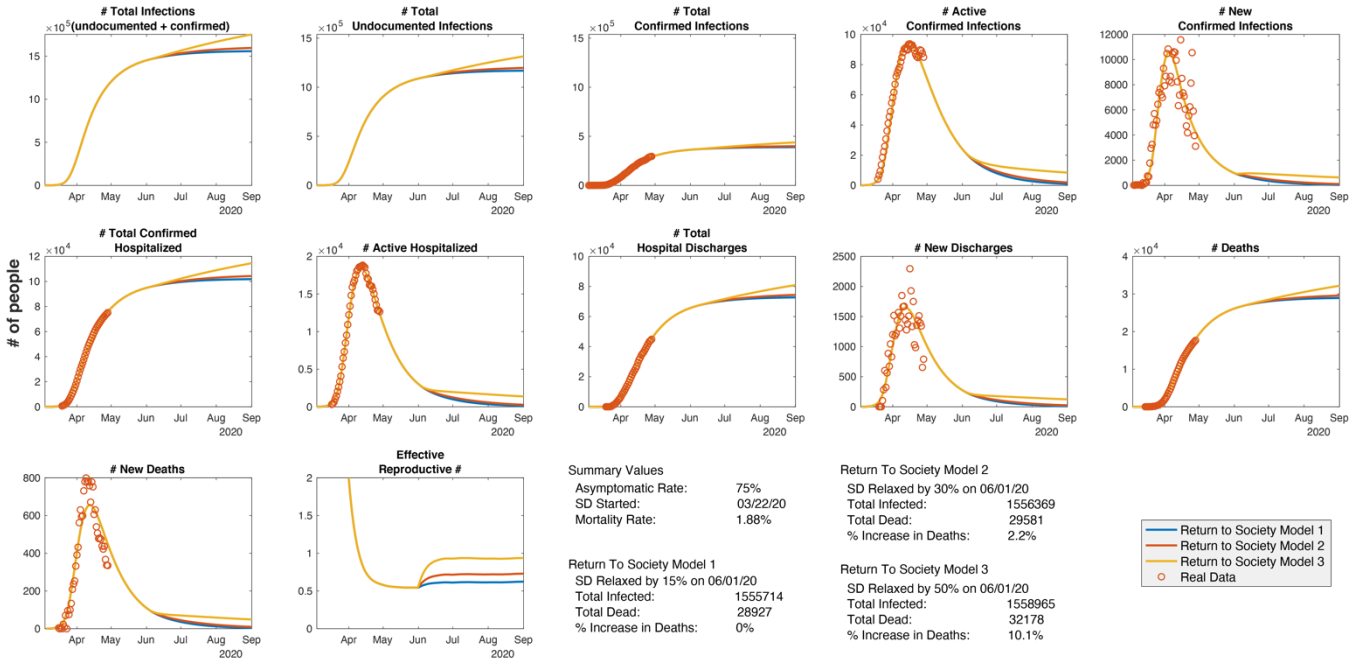

Figure S6. Short-term effects of relaxed social distancing in NYS, comprehensive outputs, related to Figure 2.

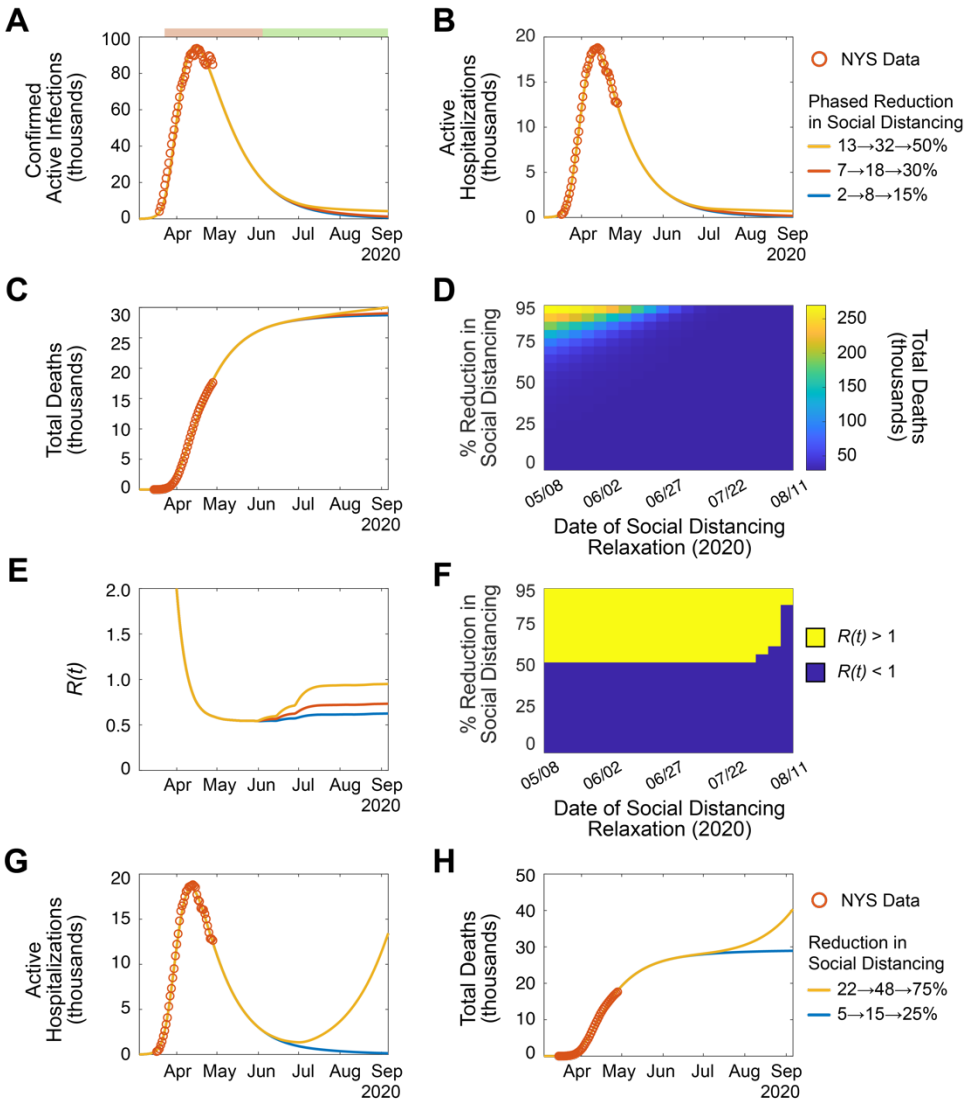

Figure S7. Short-term effects of phased relaxed social distancing in NYS, related to Figure 2. (A-F). Simulation of SARS-CoV-2 transmission dynamics in the presence of social distancing measures through September 1, 2020. Periods of social distancing signified as in (A) top: pink, increased social distancing; green, relaxed social distancing. Orange circles, NYS SARS-CoV-2 data. Lines, simulated projection of reduced social distancing starting June 1, 2020. A. Active confirmed infections. B. Active hospitalizations. C. Cumulative deaths. D. Heatmap displaying the effect of social distancing magnitude and date of reduction on the number of cumulative deaths. E. *R(t)*. F. Categorical heatmap displaying the effect of social distancing magnitude and date of reduction on *R(t)* > 1 (yellow, *R(t)*> 1; blue *R(t)*< 1). (G-H). Simulation of extreme reduction of social distancing on June 1, 2020. G. Active hospitalizations. H. Cumulative deaths.

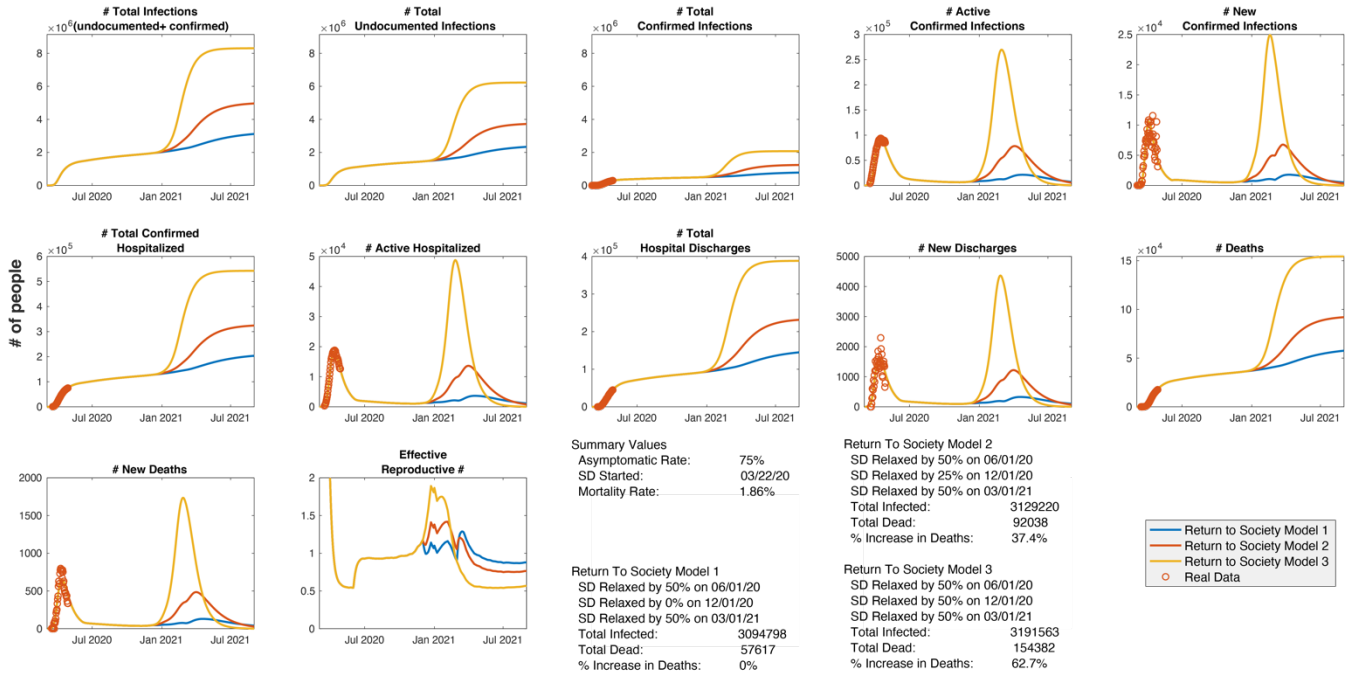

Figure S8. Recurrent outbreak of SARS-CoV-2 in NYS in early 2021, comprehensive outputs, related to Figure 3.

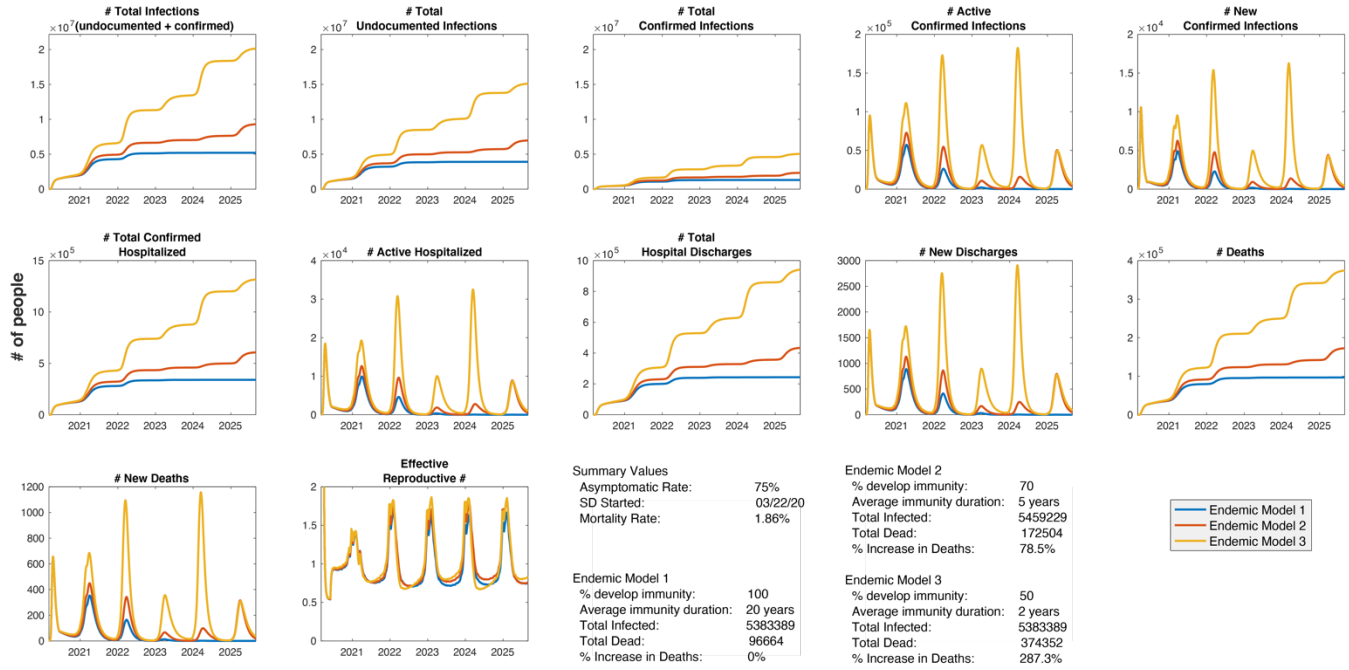

Figure S9. The endemic potential of SARS-CoV-2 depends on immunity, comprehensive outputs, related to Figure 4.

SUPPLEMENTARY REFERENCES

1. Coleman TF, Li Y. On the convergence of interior-reflective Newton methods for nonlinear minimization subject to bounds. Mathematical Programming. 1994;67(1-3):189-224. doi: 10.1007/bf01582221.

2. Kennedy J, Eberhart. R. Particle Swarm Optimization. Proceedings of the IEEE International Conference on Neural Networks. 1995:1942–5.

3. Sobol IM. On sensitivity estimation for nonlinear mathematical models. Matem Mod. 1990;2(1):112-8.

4. Diekmann O, Heesterbeek JA, Metz JA. On the definition and the computation of the basic reproduction ratio R0 in models for infectious diseases in heterogeneous populations. J Math Biol. 1990;28(4):365-82. Epub 1990/01/01. doi: 10.1007/BF00178324. PubMed PMID: 2117040.

5. Heffernan JM, Smith RJ, Wahl LM. Perspectives on the basic reproductive ratio. J R Soc Interface. 2005;2(4):281-93. Epub 2006/07/20. doi: 10.1098/rsif.2005.0042. PubMed PMID: 16849186; PubMed Central PMCID: PMCPMC1578275.

6. New York State Statewide COVID-19 Testing [Internet]. 2020. Available from: https://health.data.ny.gov/Health/New-York-State-Statewide-COVID-19-Testing/xdss-u53e.

7. QuickFacts United States [Internet]. 2019 [cited 2019]. Available from: https://www.census.gov/quickfacts/.

8. Guan WJ, Ni ZY, Hu Y, Liang WH, Ou CQ, He JX, et al. Clinical Characteristics of Coronavirus Disease 2019 in China. N Engl J Med. 2020;382(18):1708-20. Epub 2020/02/29. doi: 10.1056/NEJMoa2002032. PubMed PMID: 32109013; PubMed Central PMCID: PMCPMC7092819.

9. Li Q, Guan X, Wu P, Wang X, Zhou L, Tong Y, et al. Early Transmission Dynamics in Wuhan, China, of Novel Coronavirus-Infected Pneumonia. N Engl J Med. 2020;382(13):1199-207. Epub 2020/01/30. doi: 10.1056/NEJMoa2001316. PubMed PMID: 31995857; PubMed Central PMCID: PMCPMC7121484.

10. Lauer SA, Grantz KH, Bi Q, Jones FK, Zheng Q, Meredith HR, et al. The Incubation Period of Coronavirus Disease 2019 (COVID-19) From Publicly Reported Confirmed Cases: Estimation and Application. Ann Intern Med. 2020. Epub 2020/03/10. doi: 10.7326/M20-0504. PubMed PMID: 32150748; PubMed Central PMCID: PMCPMC7081172.

11. Goyal P, Choi JJ, Pinheiro LC, Schenck EJ, Chen R, Jabri A, et al. Clinical Characteristics of Covid-19 in New York City. N Engl J Med. 2020. Epub 2020/04/18. doi: 10.1056/NEJMc2010419. PubMed PMID: 32302078; PubMed Central PMCID: PMCPMC7182018.

12. The Covid Tracking Project: New York State [Internet]. 2020 [cited 2020]. Available from: https://covidtracking.com/data/state/new-york.

13. Bendavid E, Mulaney B, Sood N, Shah S, Ling E, Bromley-Dulfano R, et al. COVID-19 Antibody Seroprevalence in Santa Clara County, California. medRxiv. 2020:2020.04.14.20062463. doi: 10.1101/2020.04.14.20062463.

14. Sutton D, Fuchs K, D'Alton M, Goffman D. Universal Screening for SARS-CoV-2 in Women Admitted for Delivery. N Engl J Med. 2020. Epub 2020/04/14. doi: 10.1056/NEJMc2009316. PubMed PMID: 32283004; PubMed Central PMCID: PMCPMC7175422.

15. Cuomo A. Video, Audio, Photos & Rush Transcript: Amid Ongoing COVID-19 Pandemic, Governor Cuomo Announces State Health Department Will Partner with Attorney General James to Investigate Nursing Home Violations: Pressroom, NYS Governor's Press Office; 2020 [cited 2020 4/23/2020]. Available from: https://www.governor.ny.gov/news/amid-ongoing-covid-19-pandemic-governor-cuomo-announces-state-health-department-will-partner.

16. Callow KA, Parry HF, Sergeant M, Tyrrell DA. The time course of the immune response to experimental coronavirus infection of man. Epidemiol Infect. 1990;105(2):435-46. Epub 1990/10/01. doi: 10.1017/s0950268800048019. PubMed PMID: 2170159; PubMed Central PMCID: PMCPMC2271881.

17. Chan KH, Chan JF, Tse H, Chen H, Lau CC, Cai JP, et al. Cross-reactive antibodies in convalescent SARS patients' sera against the emerging novel human coronavirus EMC (2012) by both immunofluorescent and neutralizing antibody tests. J Infect. 2013;67(2):130-40. Epub 2013/04/16. doi: 10.1016/j.jinf.2013.03.015. PubMed PMID: 23583636; PubMed Central PMCID: PMCPMC7112694.